

# Effects of Distance Uncertainties on Determinations of the Galaxy Peculiar Velocity Field

Nelson Padilla, Manuel Merchán<sup>1</sup> and Diego G. Lambas.<sup>2</sup>

Grupo de Investigaciones en Astronomía Teórica y Experimental, IATE, Observatorio Astronómico,  
Laprida 854, 5000 Córdoba Argentina

## ABSTRACT

Galaxy distance indicators are subject to different uncertainties and biases which may reflect in the peculiar velocity field. In this work, we present different statistical analysis applied to peculiar velocities of samples of galaxies and mock catalogs taken from numerical simulations considering these observational effects. Our statistical studies comprise the mean relative velocity and velocity correlation for pairs of galaxies as a function of separation, and a bulk flow analysis determined on spheres of  $10h^{-1}$  Mpc radius. In order to test the statistical analysis we use COBE normalized CDM numerical simulations with different density parameters and cosmological constant and take into account the Tully-Fisher (TF) scatter and a possible TF zero-point offset, as well as variations in the results of the simulations arising from different observer positions. We compare the results of the mock catalogs with samples of spiral galaxies taken from the Mark III catalog. The results of our analysis indicate the importance of errors in deriving the density parameter  $\Omega$  from statistics applied to the observational data and it is found that large values  $\Omega \geq 0.8$  may be derived from the analysis if errors are not taken into account. However, the observed value of the TF scatter ( $\simeq 0.35$  mag) make CDM models with  $\Omega > 0.6$ , inconsistent with the statistical tests involving relative velocities. A suitable agreement is found for models with  $\Omega \leq 0.6$ , although requiring a TF zero-point offset of the order of a tenth of a magnitude to provide consistency with the observed flow coherence.

*Subject headings:* galaxies: distances — peculiar velocity field — cosmology: density parameter

## 1. Introduction

Measurements of peculiar velocities provide direct probes of the mass distribution in the Universe putting constraints on models of large-scale structure formation (e.g. Peebles, 1993, Vittorio, Juszkiewicz and Davis, 1987). Advances on new distance indicators (Djorgovski and Davis, 1987; Dressler et al., 1987a) have allowed estimates of peculiar flows in the local Universe up to  $\sim 50 - 100h^{-1}$  Mpc (see Giovanelli, 1997, or Strauss and Willick, 1995 for a review). The results from using elliptical galaxies (Dressler et al., 1987b) suggest a large coherence length and amplitude of the local peculiar velocity field. The results from analysis of 1,355 spirals using the Tully-Fisher relation to determine distances (Mathewson, Ford and Buchorn, 1992) would lead to an even larger coherence length and a similar amplitude. Other samples are also in agreement with the Great Attractor findings (Willick, 1990). In a more controversial finding Postman and Lauer (1995) find

---

<sup>1</sup>CONICOR, Córdoba, Argentina

<sup>2</sup>CONICET, Argentina

from analysis of clusters of galaxies that the peculiar flows can be coherent over a much larger scale than the Great Attractor findings. All the results indicate significant deviations from the Hubble flow with a large coherence length.

Since peculiar velocities probe the mass distribution and also depend on the density parameter  $\Omega$  one can determine the latter by comparing the mass distribution implied by the velocity field with the observed distribution of galaxies. The density parameter is thus determined to within the uncertainty of the bias factor  $b$  by determining the factor  $\Omega^{0.6}/b$ . Other analysis of the peculiar velocity information may be applied in order to obtain the parameter  $\Omega$ . Bertschinger & Dekel (1989) developed the POTENT method whereby the mass distribution is reconstructed by using the analog of the Bernoulli equation for irrotational flows. They used the method to analyze to great detail the peculiar velocity field out to about  $60h^{-1}\text{Mpc}$  (Bertschinger et al., 1989). Dekel et al. (1993) compared the previously determined velocity field with the observed distribution of galaxies and concluded that the best fit is with  $\Omega^{0.6}/b \simeq 1$ . A similar analysis can be applied to the components of the velocity tensor  $U_{ij}$  (Gorski, 1988; Groth, Juszkiewicz and Ostriker, 1989). Recently, Kashlinsky (1997) has analyzed this tensor for the MarkIII peculiar velocity data to reconstruct the large-scale power spectrum obtaining consistency within the CDM model with  $\sigma_8\Omega^{0.6} \simeq 0.8$ . In a similar study Zaroubi et al. (1997) obtain a different result  $\sigma_8\Omega^{0.6} \simeq 0.35$  indicating the need of further analysis.

In this paper we study the peculiar velocity field through a statistical analysis of COBE normalized CDM numerical simulations and observational data taken from the Mark III catalog. Our comparison of models and observations take into account observational uncertainties and possible biases, and variations of the results according to different observers in fully non-linear numerical simulations.

## 2. Data

We use the Mark III catalog (Willick et al., 1995; Willick et al., 1996; Willick et al., 1997) as a suitable data set to analyze the peculiar velocity flow. This Catalog lists Tully-Fisher and  $Dn - \sigma$  distances and radial velocities for spiral, irregular, and elliptical galaxies. In our analysis we have used only spiral galaxies given their large number and smooth spatial distribution (see Table 1).

The velocity parameter  $\eta = \text{Log}\Delta V - 2.5$  is determined either from HI profiles or from optical  $H_\alpha$  rotation curves. The TF relations and their corresponding scatters for the different samples of spiral galaxies

Table 1. Observations: The Mark III spirals

Subsample	$N^\circ$ of Gx.	TF relation	$\sigma_{TF}$
Aaronson et al. Field	359	$M_H = -5.95 + 10.29\eta$	0.47
Mathewson et al. (1992)	1355	$M_I = -5.79 + 6.8\eta$	0.43
Willick, Perseus Pisces (1991)	383	$M_r = -4.28 + 7.12\eta$	0.38
Willick, Cluster Galaxy (1991)	156	$M_r = -4.18 + 7.73\eta$	0.38
Courteau-Faber (1993)	326	$M_r = -4.22 + 7.73\eta$	0.38
Han-Mould et al., Cl. Gx. (1992)	433	$M_I = -5.48 + 7.87\eta$	0.4

are given by Willick et al., 1997 and are shown in Table 1, where the absolute magnitude  $M$  satisfies  $M = m - 5 \log cz$ . The galaxy apparent magnitudes  $m$  of the Tully-Fisher distances are corrected for Galactic extinction, inclination and redshift (see Willick et al. 1997 for details).

The selection bias in the calibration of the forward TF relation can be corrected once the selection function is known. But then, the TF inferred distances and the mean peculiar velocities suffer from Malmquist bias. Suitable procedures to consider these biases, induced both by inhomogeneities and selection function, have been discussed (see for instance /citefreud95 and references therein) where the spatial distribution, selection effects and observational uncertainties are realistically modeled through Monte-Carlo simulations. We have used in our analysis forward TF distances, fully corrected for Inhomogeneous Malmquist Bias (Willick et al., 1995, Willick et al., 1996, Willick et al., 1997). Nevertheless we have found that the results of the statistics studied in this work do not change significantly if inverse TF distances are used as it will be discussed below.

Radial velocities used to infer the peculiar velocity of the galaxies are referred to the Cosmic Microwave Background frame. It should be remarked that galaxy distance estimates are subject to errors due to the scatter in the TF relation (Mo et al., 1997; Willick, 1991; Mathewson, Ford and Buchorn, 1992) and uncertainties of the TF zero-point (Shanks, 1997; Willick, 1991). Also, the possible presence of a small fraction of spurious velocities in the data induced by either galaxy peculiarities or observational errors in distance estimates (Jacobi, 1992) should be taken into account.

### 3. Numerical Simulations

The N-body numerical simulations were performed using the Adaptive Particle-Particle Particle-Mesh (AP3M) code developed by Couchman (1991). Initial conditions were generated using the Zeldovich approximation and correspond to the adiabatic CDM power spectrum with different values of  $\Omega$  and  $\Omega_\Lambda$ . We have adopted the analytic fit to the CDM power spectrum given by Sugiyama (1995):

$$P(k) \propto \frac{k}{[+3.89q + (16.1q)^2 + (5.46q)^3 + (6.71q)^4]^{1/2}} \left( \frac{\ln(1 + 2.34q)}{2.34q} \right)^2 \quad (1)$$

where  $q = \frac{k}{\Gamma h} \text{Mpc}$ ,  $\Gamma = \frac{k\theta^2}{h \exp(-\Omega_B - \sqrt{h/0.5\Omega_B/\Omega})}$ ,  $\theta$  is the microwave background radiation temperature in units of  $2.7K$ , and  $\Omega_B = 0.0125h^{-2}$  is the value of the baryon density parameter given by nucleosynthesis. The normalization of the CDM power spectrum is imposed by COBE measurements using values of  $\Omega$ ,  $\sigma_8$  (defined as the mass fluctuations in spheres of radius =  $8Mpc h^{-1}$ ) and  $h$  (the Hubble constant in units of  $100 km/s/Mpc$ ) chosen from Table 1 of Górski et al., (1995) and corresponding to ages of the universe  $t_0 \simeq 12$  and  $14$  Gyr for the  $\Lambda = 0$  and  $\Lambda \neq 0$  models respectively. The computational volume is a periodic cube of side length  $300$  Mpc. We have followed the evolution of  $N = 5 \times 10^5$  particles with  $64$  grid per side and a maximum level of refinements of  $4$ . The resulting mass per particle is  $4.11 \times 10^{12} \Omega_0 h^{-1} M_\odot$ . The initial conditions correspond to redshift  $z = 10$  and the evolution was followed using  $1000$  steps. At the final step ( $z = 0$ ) the linear extrapolated value of  $\sigma_8$  is compatible with the normalization imposed by observed temperature fluctuations in the cosmic background. In Table 2 are resumed the principal characteristics of the different numerical simulations.

#### 4. Statistical Analysis Outline

In this section we outline the main statistical procedures followed to analyze the galaxy peculiar velocity field, as well as the comparison of model results and the observations.

Our statistics are based on a direct comparison between the observations and mock catalogs derived from the numerical simulations. The COBE normalized CDM models studied require no strong bias, so we have adopted  $b = (\delta M/M)/(\delta N/N) = 1$  in the simulations. This assumption is not crucial in the results of our studies since we have analyzed mock catalogs with different bias parameters  $.75 < b < 1.35$  finding no significant differences in the statistical results presented in this work.

Also, we have studied the effects produced by different limiting radial distances in our comparison of models and observations by setting two different catalog depth limits  $d_{lim} = 5000$ , and  $10000 \text{ km/s}$  (1764 and 2854 galaxies respectively).

We have considered an analysis of bulk motions as measured by the distribution of peculiar velocities of neighbor galaxies using mean values, dispersions and Kurtosis (as a suitable parameter to measure departures from gaussianity) to describe the velocity distribution. We define shells of radius  $\Delta r < 2000 \text{ km/s}$  and width  $\delta r = 200 \text{ km/s}$  centered in each of the galaxies of the sample and we compute the difference between each galaxy radial velocity in the shell ( $v_b$ ) and the mean motion of the galaxies in a sphere of radius  $10 h^{-1} \text{ Mpc}$  ( $\bar{v}_a$ ). We compute the dispersion and kurtosis (D, K respectively) of these relative velocities across the shells as a function of  $\Delta r$ .

$$D = \sqrt{\langle (v_b - \bar{v}_a)^2 \rangle} \quad (2)$$

$$K = \frac{(v_b - \bar{v}_a)^4}{D^2} - 3 \quad (3)$$

We have also studied the distribution of the radial velocity moduli of the shells in order to derive a quantity related to the coherence of the flow. We have computed the ratio (M) of the mean of this distribution to the dispersion D described in the preceding paragraph. The parameter M provides a useful information on the coherence of the velocity flow by measuring the mean systematic to random motion ratio of shells of radius  $\Delta r$  (Note that M differs from the definition of the Cosmic Mach Number given by Ostriker and Suto, 1990).

Table 2. Simulations

$\Omega$	$\Omega_\Lambda$	$h_{100}$	$\sigma_8$
0.3	0.7	0.65	1.05
0.4	0.0	0.65	0.75
0.5	0.0	0.60	0.90
0.6	0.0	0.60	1.12
0.7	0.0	0.60	1.32
0.8	0.0	0.55	1.325

$$M = \frac{\langle |v_b| \rangle}{D} \quad (4)$$

We have also provided a different statistical characterization of the peculiar velocity field through an analysis of the distribution of relative radial velocities of pairs of galaxies ( $v_b$  and  $v_a$ ) as a function of separation (for simplicity we use the same variable  $\Delta r$  as the shell radii of the previously defined statistics  $D$ ,  $K$  and  $M$ ). We have computed the corresponding dispersion (D1) and kurtosis (K1) and we calculate the average modulus of the pair peculiar velocity difference ( $\Delta V$ ). A measurement of the pairwise coherence of the flow is also provided by estimating the average of the product of radial peculiar velocities of pairs of galaxies with separation  $\Delta r$  ( $\Pi$ ).

$$D1 = \sqrt{\langle (v_b - v_a)^2 \rangle} \quad (5)$$

$$K1 = \frac{\langle (v_b - v_a)^4 \rangle}{D^2} - 3 \quad (6)$$

$$\Delta V = \langle |v_a - v_b| \rangle \quad (7)$$

$$\Pi = \sqrt{\langle v_a v_b \rangle} \quad (8)$$

The D1 parameter corresponds to the mean pairwise velocity dispersion usually estimated from the distortion of the correlation function in redshift-space. It should be noted, however, that the D1 results obtained from the peculiar velocity data would not be directly comparable with the correlation function distortion findings. This is mainly due to the presence of biases and uncertainties in the peculiar velocity data and the different hypotheses adopted in the redshift-space correlation analysis (see for instance Jing et al., 1998).

We have considered 100 random observers in each numerical simulation by defining cones with different positions and orientations in our computational volume. Also, given the presence of a strong radial gradient in the data we have attempted to study its possible effects on the determinations of velocity statistics. The observed radial gradient corresponds approximately to a selection bias due to a magnitude limit cutoff. This can be seen from the observed distribution of absolute magnitudes which is nearly gaussian with mean  $\simeq M^*$  (the knee of the Luminosity Function) and  $\sigma \simeq 1.5mag$ . Nevertheless, for our statistical purposes it is not necessary to adopt a Monte-Carlo model using the Galaxy Luminosity Function in the simulations. This is mainly due to the lack of strong dependence of observed galaxy luminosities with environment. Therefore, it suffices to reproduce the observed radial gradient in the numerical models through a Monte-Carlo rejection algorithm. Accordingly, we use this procedure to reproduce in the mock catalogs derived from the numerical simulations, the observed galaxy radial gradient. Furthermore, we restrict the resulting number of particles of the mock catalogs to be of the order of the number of galaxies in the observational sample.

We find that the radial gradient is very important since it significantly changes the results of the statistics when errors are included.

In order to quantify the effects of observational errors in galaxy distance estimates we have considered gaussian errors in the galaxy absolute magnitudes of the TF relation with dispersion  $\Delta M = 0.35 mag$  corresponding to relative errors in distances  $\simeq 17\%$  (Mathewson, Ford and Buchorn, 1992; Willick, 1991). Namely, we assign to each particle in the mock catalog a new distance  $d_{new} = d * (1 + s)$  where  $s$  is taken from a gaussian distribution with dispersion corresponding to the TF uncertainty. Then, as the particle peculiar velocities are inferred from the galaxy redshift and distance,  $v_{new} = v - d * s$ .

We have also explored the effects produced by a possible TF zero-point offset (either positive or negative) in the statistical results. In our analysis we have considered absolute magnitude offsets  $|\Delta M| = 0.15 \text{ mag}$  corresponding to twice the *rms* uncertainty derived in Willick, 1991, and have been adopted to test their effects on the statistics.

The mean galaxy peculiar velocities are enhanced due to the scatter of the TF relation by a factor approximately proportional to their distances. Since our statistics deal with small angular separations between the galaxies, the TF scatter will mostly affect the results involving relative radial peculiar velocities. On the other hand, the coherence of the flow would be significantly enhanced by an offset in the TF zero-point (either positive or negative) due to the systematic motion of the galaxies added to the true velocity field. We have also considered the effects of a fraction of spuriously high peculiar velocities in the Mark III catalog. To constraint the number of these systematically large velocities in the data we have added to the peculiar velocities of a given fraction of particles of the mock catalogs a velocity taken from an even probability distribution  $p = \text{constant}$  within  $3\sigma$  and  $6\sigma$ , and zero elsewhere ( $\sigma$  is the dispersion of the observed distribution of peculiar velocities). The kurtosis parameter involves the 4-th power of the difference between the observed value of a given quantity and the mean of its distribution (see eq. 3 or eq. 6) providing a useful test for the presence of exceedingly large velocities. From a comparison of observation and model kurtosis values we may pose suitable constrains to the fraction of spurious peculiar velocities in the observational data.

## 5. Results

We have computed the different statistics  $K$ ,  $K1$ ,  $D$ ,  $D1$ ,  $\Delta V$ ,  $\Pi$ , and  $M$  in both the numerical models and the observational samples of spirals from Mark III for 8 radial bins. In order to avoid numerical resolution problems in the simulations we analyze relative separations  $\Delta r > 400 \text{ km/s}$ .

In figure 1 we show the kurtosis test results  $K$  (eq. 3) and  $K1$  (eq. 6) for the observations (solid lines) and the models.

The results for the open  $\Omega = 0.4$  model without considering peculiar velocity errors are displayed with dashed lines in figure 1a and 1c while the effects of the TF scatter and zero-point offset may be appreciated in figures 1b and 1d (dotted and dashed lines respectively) as well as the effects produced by a percentage of exceedingly large peculiar velocities  $v = 3\sigma$  to  $6\sigma$  (long-dashed lines). It can be seen in this figure the lack of importance of the TF scatter and zero point offset ( $0.35 \text{ mag}$  and  $+0.15 \text{ mag}$  respectively) in contrast to the strong effect of spurious large velocities. A modest fraction ( $\simeq 2\%$ ) of such velocities produce too large values of  $K$  and  $K1$  in the models compared to observations which suggest this fraction as an upper limit for the presence of strongly biased distance estimates. Also we find similar values of  $K$  and  $K1$  for the different models indicating that kurtosis is not suitable to provide restrictions to cosmological parameters.

In figure 2 we display  $D$  (eq. 2) for the observations (solid lines) and the  $\Omega = 0.4$  and  $\Omega = 0.8$  CDM models. In figure 2a) no peculiar velocity errors are included (dashed lines  $\Omega = 0.4$  model, long dashed lines  $\Omega = 0.8$  model). In figure 2b) we show the effects of the TF scatter and zero-point offset. The dotted lines show the results of a  $\simeq 17\%$  relative distance error in the  $\Omega = 0.4$  model as expected by the TF intrinsic scatter ( $0.35 \text{ mag}$ ). Additional TF zero-point offsets  $\Delta M_0 = +0.15$  and  $-0.15 \text{ mag}$  do not significantly change the results and are shown as open and filled triangles respectively for the  $\Omega = 0.4$  model. Long dashed lines correspond to  $\Omega = 0.8$  model with TF scatter included (no TF zero-point offset). Error bars indicate the rms variation of the results from different mock catalog of the models. It can be seen in this figure

that the TF scatter strongly dominates this statistical test allowing low values of  $\Omega$  to fit the observations.

Similarly, in figure 3 we show the results of the D1 (eq. 5) test in the observational data (solid lines) and the corresponding results of the  $\Omega = 0.4$  and  $\Omega = 0.8$  CDM models. Observational errors are not included in figure 3a and TF scatter ( $\Omega = 0.4$  model, dotted lines) plus additional  $\pm 0.15$  mag TF zero-point offsets in the  $\Omega = 0.4$  model (open and filled triangles). The results for the  $\Omega = 0.8$  model with TF scatter are displayed with long dashed lines.

We show the results of the  $\Delta V$  test (eq. 7) for the  $\Omega = 0.4$  and  $\Omega = 0.8$  models in figure 4 (dotted and dashed lines respectively). In Figure 4a no errors are included in the models, and in figure 4b we have included  $0.35$  mag TF scatter and  $\pm 0.15$  mag zero-point offset with same symbols as in previous figures.

It can be appreciated by inspection to figures 2 to 4 the difficulties of matching the observations with a high density CDM model as well as the adequate fit provided by the  $\Omega = 0.4$  model (the flat  $\Omega = 0.3$  model works very good as well). It is a remarkable fact that the magnitude and shape of the observed  $D$ ,  $D1$  and  $\Delta V$  as a function of separation can be adequately reproduced in a low density CDM model when the TF scatter is taken into account.

In figure 5 are displayed  $\Pi$  (eq. 8) and  $M$  (eq. 4) for the observations and the  $\Omega = 0.4$  model. Symbols are as in previous figures, and no errors are included in the model of figure 5a, while in figure 5b we show the results with TF scatter and zero-point offsets. Both affect significantly the coherence of the velocities; TF zero-point offsets rise  $\Pi$  in a factor proportional to  $\Delta r$ ; while the scatter reduces the coherence at large separations  $\Delta r$  and increases it at small  $\Delta r$ . It is interesting to compare these results with those derived from the velocity correlation function (see for instance Strauss and Willick, 1995) where a coherence length of  $2000$  km/s is observed for the Aaronson sample of the MarkIII catalog. From our analysis we find a larger value of the coherence length  $\simeq 2800$  km/s. However we note that this spatial scale defined by a lack of velocity correlation depends on the catalog depth, and very strongly on TF scatter since at distances  $\geq 2000$  km/s, the associated uncertainties in the peculiar velocities are of comparable magnitude to the flow coherence.

In order to asses the ability of the models to reproduce the observations we calculate the frequency  $\mathcal{L}(\Omega)$  that the observational values of a statistical test are within the range of the results obtained with a large number of random observers (mock catalogs) as a function of model density parameter  $\Omega$ . Specifically, we compute

$$\chi_{obs}^2 = \sum_{\Delta r} (O_{\Delta r} - A_{\Delta r})^2 / \sigma_{\Delta r}^2$$

$$\chi_i^2 = \sum_{\Delta r} (R_{\Delta r i} - A_{\Delta r})^2 / \sigma_{\Delta r}^2$$

where R refers to the resulting value of a particular statistical test for the random  $i^{th}$  observer; and A, to the corresponding average across the ensemble of random observers. Both R and A are computed for a given model as a function of separation  $\Delta r$ ,  $\sigma_{\Delta r}^2 = \sum_i (R_{\Delta r i} - A_{\Delta r})^2 / N$ , and O corresponds to the observed value of the statistical tests under consideration.

We find that  $\chi_i^2$  has approximately a gaussian distribution with dispersion  $\sigma_i$  in the models explored,

and we therefore estimate

$$\mathcal{L}(\Omega) = \frac{1}{\sigma_i} \sqrt{\frac{2}{\pi}} \int_{\chi_{obs}^2}^{\infty} e^{-x^4/(2\pi\sigma_i^2)} d\chi^2 \quad (9)$$

as a suitable likelihood of a given model to reproduce the observed values of a particular statistical test.

For the two catalog depths analyzed  $d_{lim} = 5000 \text{ km/s}$  and  $d_{lim} = 10000 \text{ km/s}$  we find that the results of the statistics do not change strongly. Moreover, the changes in the statistics from one catalog depth to the other in the observations and in the mock catalogs are similar indicating that the conclusions derived are not depth dependent. However, the dispersion arising from different observer positions is considerably larger in the  $d_{lim} = 5000 \text{ km/s}$  case which suggests the use of the deeper sample.

We display in figure 6 the likelihood  $\mathcal{L}(\Omega)$  obtained for our different statistical tests using catalog depth  $d_{lim} = 10000 \text{ km/s}$ , and considering a  $0.35 \text{ mag}$  TF scatter (figure 6a), plus additional  $-0.15$  and  $+0.15 \text{ mag}$  zero-point offsets (figure 6b and c). From inspection to figure 6a, we note that in the absence of a TF zero-point offset the likelihood associated to  $D$  and  $\Delta V$  for models with  $\Omega > 0.6$  are  $\leq 0.1\%$ . On the other hand, the observed flow coherence as reflected in the  $\Pi$  and  $M$  tests is in better agreement with high  $\Omega$  models. The effects of a negative and positive TF zero-point offset may be appreciated in figure 6b and 6c, where it is seen that high values of  $\Omega > 0.6$  are not suitable to match the observed  $D$ ,  $D1$ , and  $\Delta V$  statistical tests, while the remaining tests do not exclude any of the models explored ( $\mathcal{L} > 10\%$ ). We find that a positive TF zero-point offset provides a better agreement between the observations and low density CDM models.

We have also analyzed the dependence of the results on the magnitude of the TF scatter. In figure 6d, we display  $\mathcal{L}$  for the  $\Delta V$  test for the  $\Omega = 0.4$ ,  $\Omega = 0.6$  and  $\Omega = 0.8$  CDM models as a function of the TF scatter  $\Delta M$ . It can be seen in the figure the strong dependence of  $\mathcal{L}$  on the assumed value of the TF scatter. For  $\Delta M > 0.3$  the  $\Omega = 0.8$  model is ruled out by this test with large confidence. On the other hand if  $\Delta M < 0.25$  the  $\Omega = 0.4$  model would be ruled out. However it should be noticed that the TF scatter of the different samples in the MarkIII catalog, are in all cases  $> 0.35$  (See Table 1), the adopted value in our analysis.

We have repeated our analysis using inverse TF distances to test possible systematic influences on the statistics. We find similar results in this case than in the case of forward distances indicating that either estimates are suitable to be used in our statistical studies.

We have also examined the effects of biasing the distribution of particles in the numerical simulations on the results of the statistics. We have biased the  $\Omega = 0.4$  model and anti-biased the  $\Omega = 0.8$  model, so that the relative galaxy number fluctuation on spheres of  $8 \text{ Mpc}$  is unity for these two models. Each particle is associated to a galaxy with probability  $\eta$  which depends on the local density. We smooth the density field calculating the mass density  $\rho$  centered at each particle within a sphere of radius  $1.5h^{-1} \text{ Mpc}$  and we adopt a simple power-law model  $\eta(\rho) = (\rho/\rho_c)^\alpha$  for the assignment of particles. We find that our results are not strongly modified for these biased models with resulting  $\mathcal{L}(\Omega)$  of the same order of magnitude. This result is important since it indicates that our conclusions regarding the value of the density parameter do not depend crucially on the adopted normalization nor on the assumption that galaxies trace the mass.



## 6. Conclusions

In this work we have attempted to assess the effects of galaxy distance uncertainties and biases on statistical tests of the peculiar velocity field using samples of spiral galaxies from the Mark III compilation and mock catalogs taken from numerical simulations. Our studies comprise relative velocity tests and pair velocity correlations as a function of separation, as well as a bulk flow analysis determined on spheres of  $10h^{-1} Mpc$  radius. We construct mock catalogs using numerical simulations corresponding to COBE normalized CDM models with different values of density parameter and cosmological constant. The models take into account the Tully-Fisher (TF) scatter and possible TF zero-point shift, as well as variations in the results of the simulations arising from different observer positions. The analysis of the departures from gaussianity of the observational velocity distributions as measured by the kurtosis tests  $K$  and  $K1$  show that only a small fraction ( $< 2\%$ ) of possible spuriously high velocities (and therefore biased distance estimates) might be present in the observational data. We find that the observed scatter of the TF relation plays a very important role when deriving constraints to the cosmological parameters. If errors in galaxy distance estimates are neglected, the observed magnitude of the  $\Delta V$  results show consistency with high density CDM models ( $\Omega > 0.8$ ). When the observed TF scatter  $\Delta M \simeq 0.35$  is taken into account a significant disagreement with observations is found for the  $\Delta V$  and  $D1$  statistics in models with  $\Omega > 0.6$ .

A possible offset in the TF zero-point used to determine the distances of the galaxies in the observational data artificially enhance velocity correlations ( $\Pi$  and  $M$  statistics). Due to this fact, if zero-point offsets of the order of a tenth of a magnitude are considered, the CDM models explored provide a more satisfactory fit to observations in these tests.

The results presented in this work are not sensitive to sample variations. We have applied the same statistical tests to the subsample corresponding to Mathewson data and we find similar results than those of the total sample. It should be noted that the variations on the statistics arising from different observers are significantly enhanced when errors on the peculiar velocities are included. This fact make more difficult the distinction between the models. Error bars in figures 1 to 5 show the variations of the results arising from different observer positions in the models and serve as a test for the dependence of the observational results on our particular position in space. In our analysis of biased models we have not found relevant differences in the results of the statistical analysis of samples with different density thresholds. The selection of low (high) density particles in the simulations does not produce very relevant effects in the statistics although lower (higher) values of  $\Pi$  and  $\Delta V$  are observed due to the oversampling (undersampling) of high density particles where random motions dominate. Finally when comparing models and observations, we find that neither the  $K$ ,  $K1$ ,  $M$ , nor  $\Pi$  statistical tests are sensitive to the density parameter of the models.

We find crucial to consider properly the intrinsic scatter of the Tully-Fisher relation in studies of the peculiar velocity field. Although low values of the density parameter  $\Omega < 0.6$ , are favored by our statistical analysis  $D1$  and  $\Delta V$  when this scatter is taken into account  $\pm 0.15 mag$  zero-point offsets in the TF relation are required in order to provide the observed values of  $\Pi$  and  $M$  statistics in the models explored. A positive TF zero-point offset of this magnitude would imply lower values of the Hubble constant which may be worth to consider in a controversial topic (see for instance Shanks, 1997 and Theureau (1997) and references therein).

## 7. Acknowledgements

We thank H. Couchmann for kindly providing the AP3M code. We have benefited from helpful discussions with Jim Peebles and Julio Navarro.

This work was supported by the Consejo de Investigaciones Científicas y Técnicas de la República Argentina, CONICET, the Consejo de Investigaciones Científicas y Tecnológicas de la Provincia de Córdoba, CONICOR, and the Fundación Antorchas, Argentina.

## REFERENCES

- Bertschinger, E. and Dekel, A. 1989, ApJ, 336, L5.
- Bertschinger, E. et al. 1989, ApJ, 364, 370.
- Couchman, H.M.P. 1991, ApJ, 368, L23
- Dekel, A. et al. 1993, ApJ, 412, 1.
- Djorgovski, G. and Davis, M. 1987, ApJ, 313, 59.
- Dressler, A. et al. 1987a, ApJ, 313, 42.
- Dressler, A. et al. 1987b, ApJ, 313, L37.
- Freudling, W. et al., 1995, AJ, 110, 920F.
- Giovanelli, R. in Critical Dialogues in Cosmology, Ed., N. Turok, 1997, World Scientific.
- Gorski, K. 1988, ApJ, 332, L7.
- Górski, K.M., Ratra, B., Sugiyama, N. & Branday 1995, ApJ, 444, L5.
- Groth, E., Juszkievicz, R. and Ostriker, J. 1989, ApJ, 346, 558.
- Jacoby et al. 1992, PASP, 104, 599.
- Jing, Y. P., Mo, H. J., Boerner, G., accepted for publication on ApJ, 494, 1998.
- Kashlinsky, A. 1997, ApJ, in press, preprint astro-ph/9705002.
- Mathewson, D., Ford, V.L. and Buchorn, M. 1992, ApJ, 389, L5.
- Mo, H.J., Mao, S., White, S.D.M., 1997, preprint (astro-ph/9707093).
- Ostriker, J. P., Suto, Y., 1990, ApJ, 348, 378.
- Peebles, P.J.E., Principles of Physical Cosmologies, Princeton University Press, 1993.
- Postman, M. and Lauer, T.R. 1995, ApJ, 440, 28.
- Shanks, T., 1997, preprint (astro-ph/9702148).
- Strauss, M. and Willick, J.A. 1995, Phys.Reports, 261, 271.
- Sugiyama, N. ApJS, 100, 281.
- Theureau et al., A&A, 332, 730.
- Vittorio, N., Juszkievicz, R. and Davis, M. 1987, Nature, 323, 132.
- Willick, J. 1990, ApJ, 351, L5.
- Willick, J. 1991, Doctoral Thesis.
- Willick, J.A., Courteau, S., Faber, S.M., Burstein, D., & Dekel, A., ApJ, 446, 1, 1995

Willick, J.A., Courteau, S., Faber, S.M., Burstein, D., Dekel, A., & Kolatt, T., ApJ, 457, 460, 1996

Willick, J.A., Courteau, S., Faber, S.M., Burstein, D., Dekel, A., & Strauss, M.A., ApJS in press (astro-ph/9610200), 1997

Zaroubi, S., Zehavi, I., Dekel, A., Hoffman, Y. and Kolatt, T. 1997, ApJ, in press, preprint astro-ph/9610226.

Figure 1

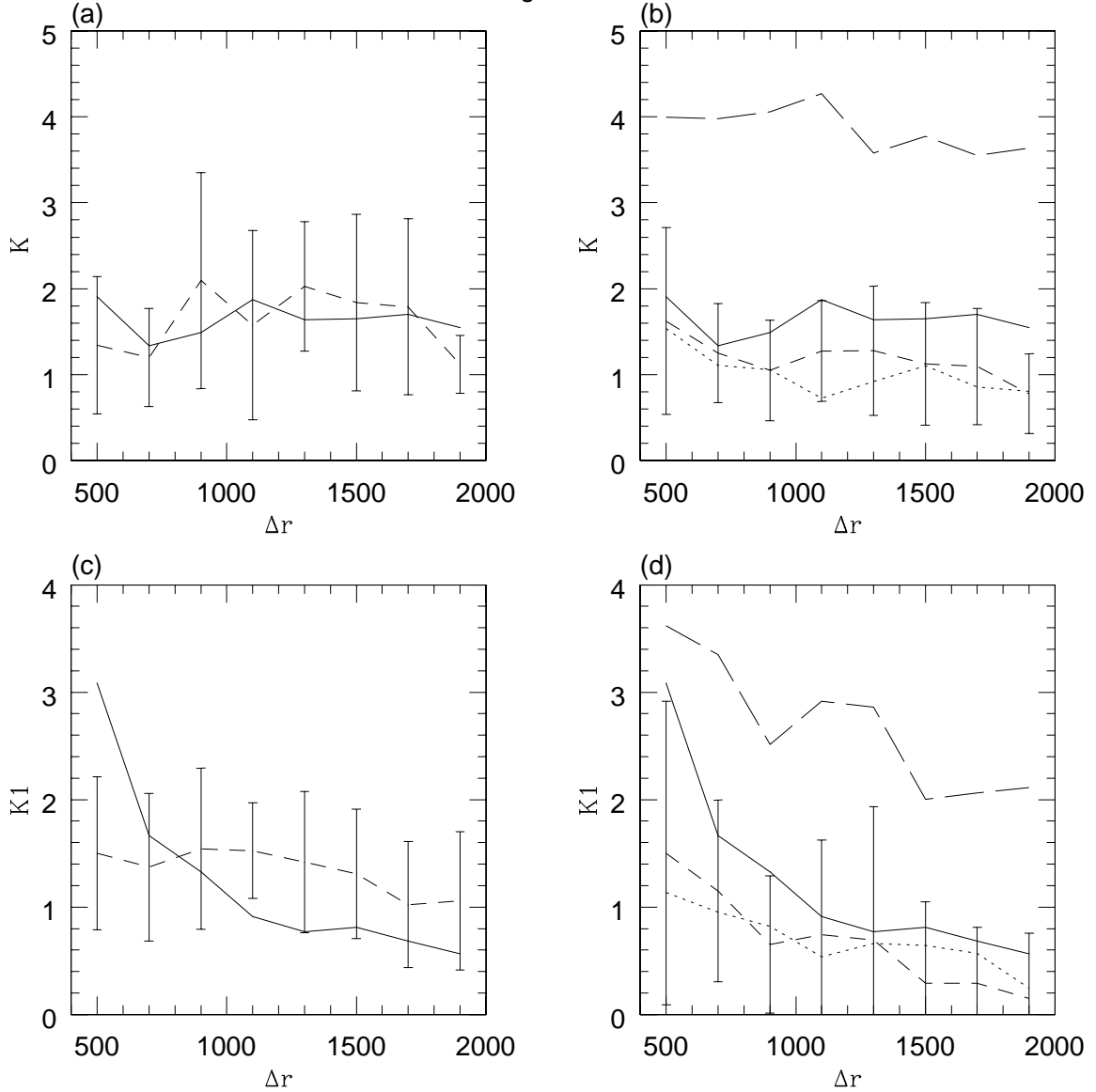


Fig. 1.— Kurtosis tests  $K$  and  $K1$ . Solid lines show the observed values. Left panels display the results with no errors included in the  $\Omega = 0.4$  CDM model. Right panels: dotted lines show the effects of a TF scatter, dashed lines the addition of a  $+0.15\text{mag}$  TF zero-point offset. The long dashed lines show the expected  $K$  and  $K1$  values under the assumption that 2% of the galaxies have spurious peculiar velocities ( $3$  to  $6\sigma$  from the mean) due to wrong distance determinations. Error bars indicate the rms variation arising from different observer positions in the  $\Omega = 0.4$  model. To avoid confusion in the figures we display only the cases where no errors are considered and where a TF scatter with additional positive TF zero-point offset is taken into account.

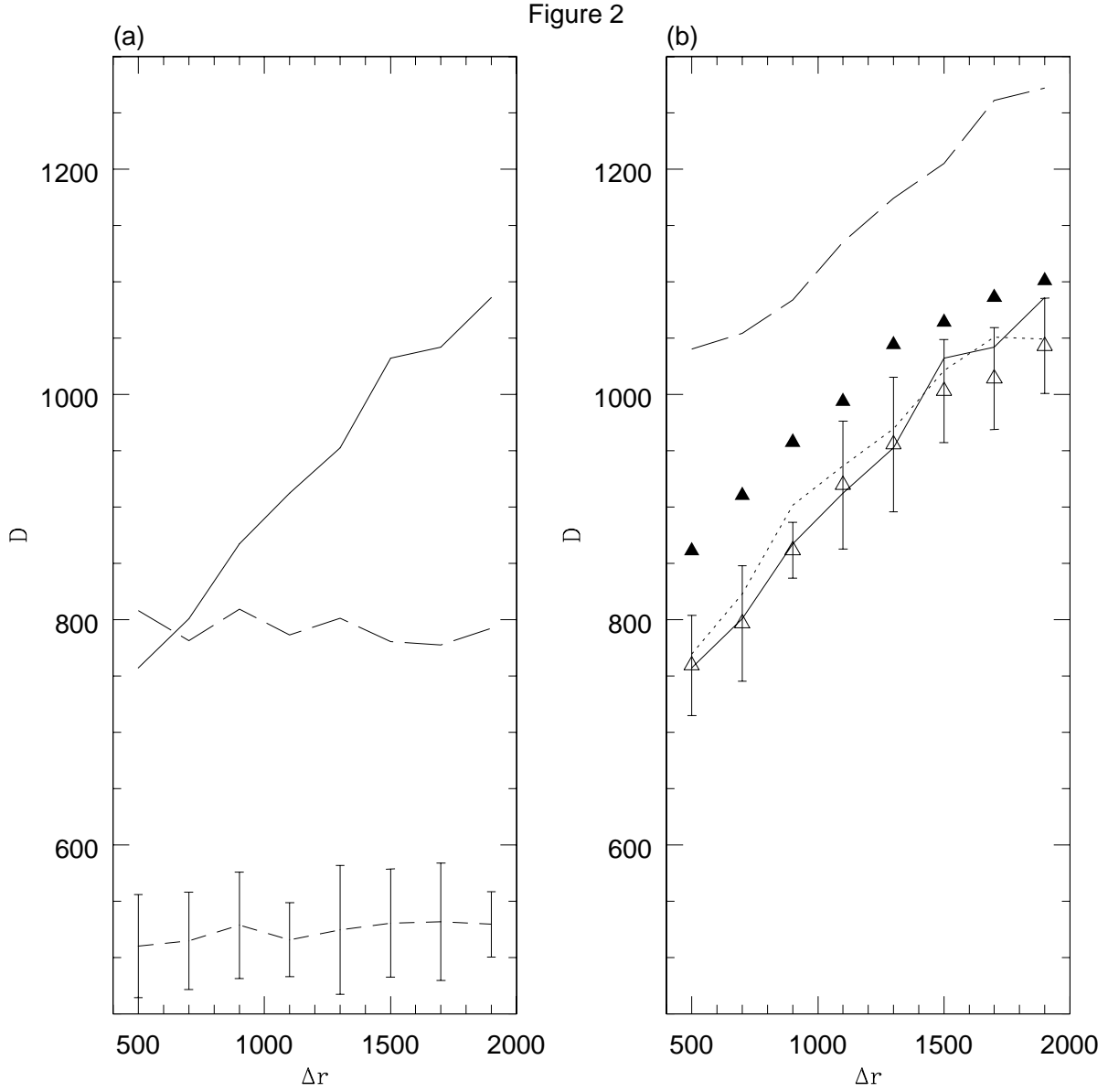


Fig. 2.— D test results. Solid lines show the observed values. Figure 2a: no errors included in the  $\Omega = 0.4$  (dashed line) and  $\Omega = 0.8$  (long-dashed line) CDM models. Figure 2b: effects of a  $0.35 \text{ mag}$  TF scatter (dotted line) and additional  $+0.15 \text{ mag}$  and  $-0.15 \text{ mag}$  TF zero-point offsets (open and filled triangles respectively) in the  $\Omega = 0.4$  CDM model. The long dashed line corresponds to the  $\Omega = 0.8$  CDM model with same TF scatter. Error bars represent the same as in figure 1.

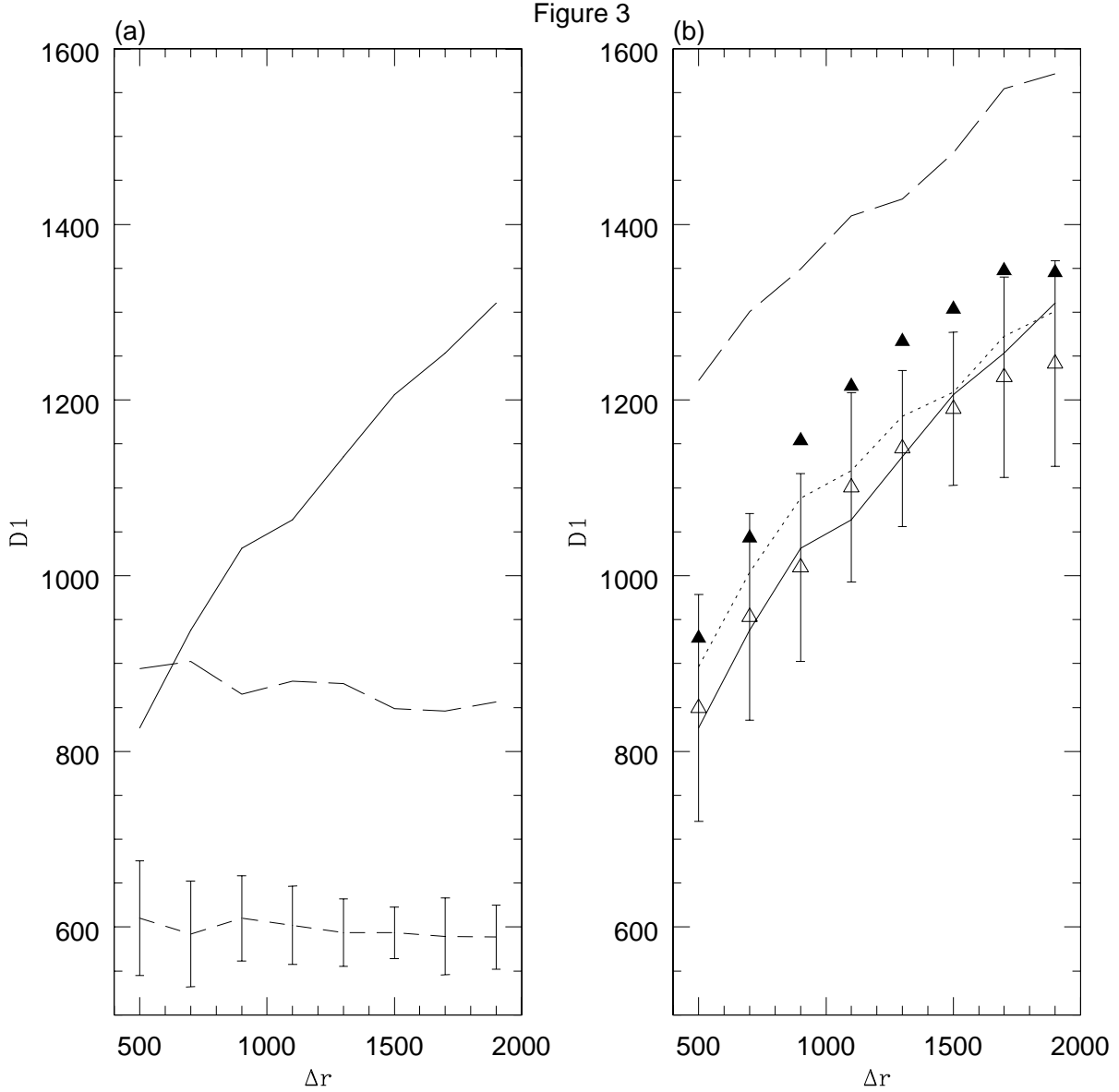


Fig. 3.— D1 test results. Solid lines show the observed values. Figure 3a: no errors included in the  $\Omega = 0.4$  (dashed line) and  $\Omega = 0.8$  (long-dashed line) CDM models. Figure 3b: effects of a  $0.35 \text{ mag}$  TF scatter (dotted line) and additional  $+0.15 \text{ mag}$  and  $-0.15 \text{ mag}$  TF zero-point offsets (open and filled triangles respectively) in the  $\Omega = 0.4$  CDM model. The long dashed line corresponds to the  $\Omega = 0.8$  CDM model with same TF scatter. Error bars represent the same as in previous figures.

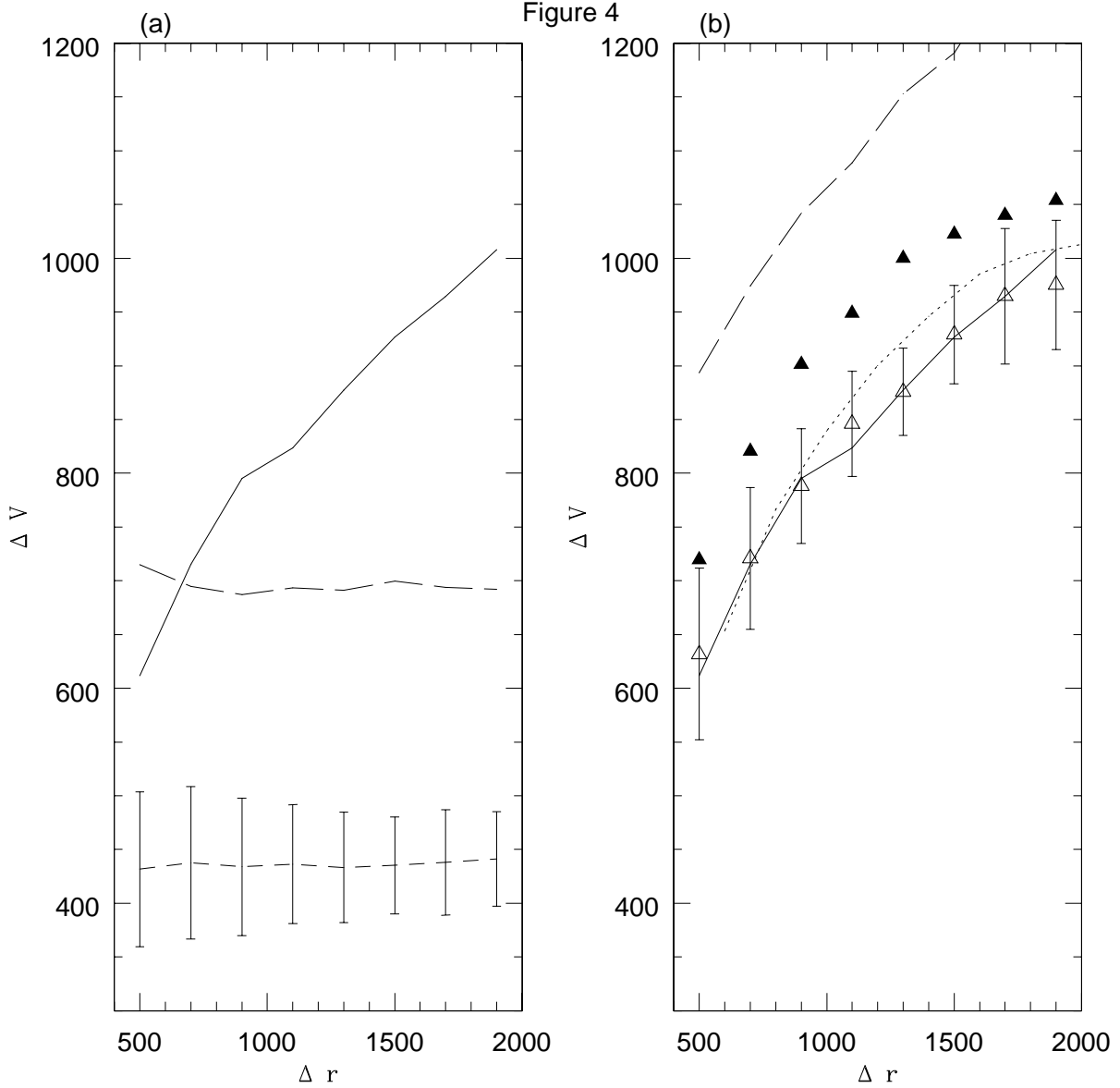


Fig. 4.—  $\Delta V$  test results. Solid lines show the observed values. Figure 4a: no errors included in the  $\Omega = 0.4$  (dashed line) and  $\Omega = 0.8$  (long-dashed line) CDM models. Figure 4b: effects of a  $0.35 \text{ mag}$  TF scatter (dotted line) and additional  $+0.15 \text{ mag}$  and  $-0.15 \text{ mag}$  TF zero-point offsets (open and filled triangles respectively) in the  $\Omega = 0.4$  CDM model. The long dashed line corresponds to the  $\Omega = 0.8$  CDM model with same TF scatter. Error bars represent the same as in previous figures.



Figure 5

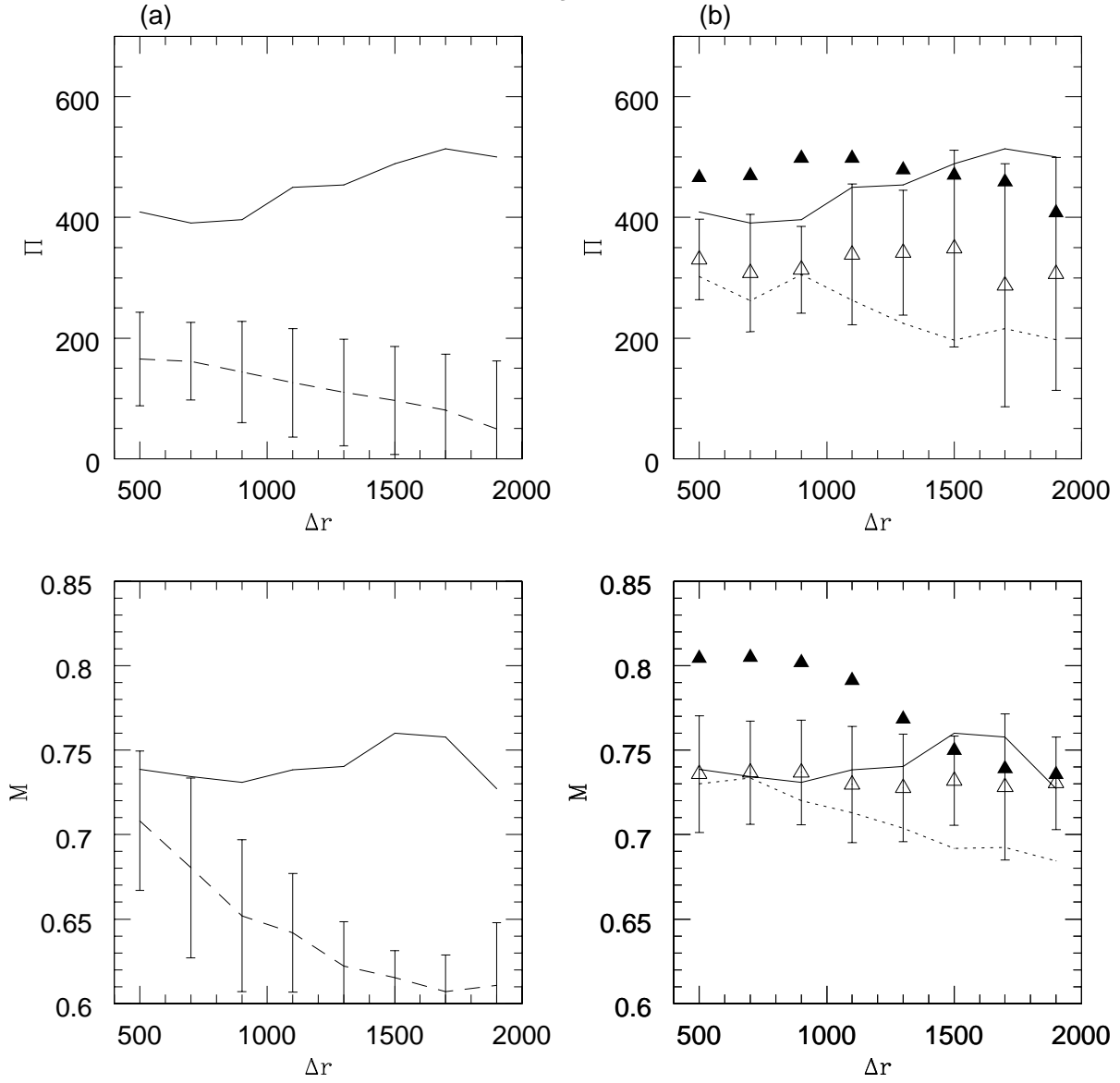


Fig. 5.—  $\Pi$  and  $M$  test results. Solid lines show the observed values. Figure 5a: no errors included in the  $\Omega = 0.4$  (dashed line). Figure 5b: effects of a  $0.35 \text{ mag}$  TF scatter (dotted line) and additional  $+0.15 \text{ mag}$  and  $-0.15 \text{ mag}$  TF zero-point offsets (open and filled triangles) in the  $\Omega = 0.4$  CDM model. Error bars represent the same as in previous figures.

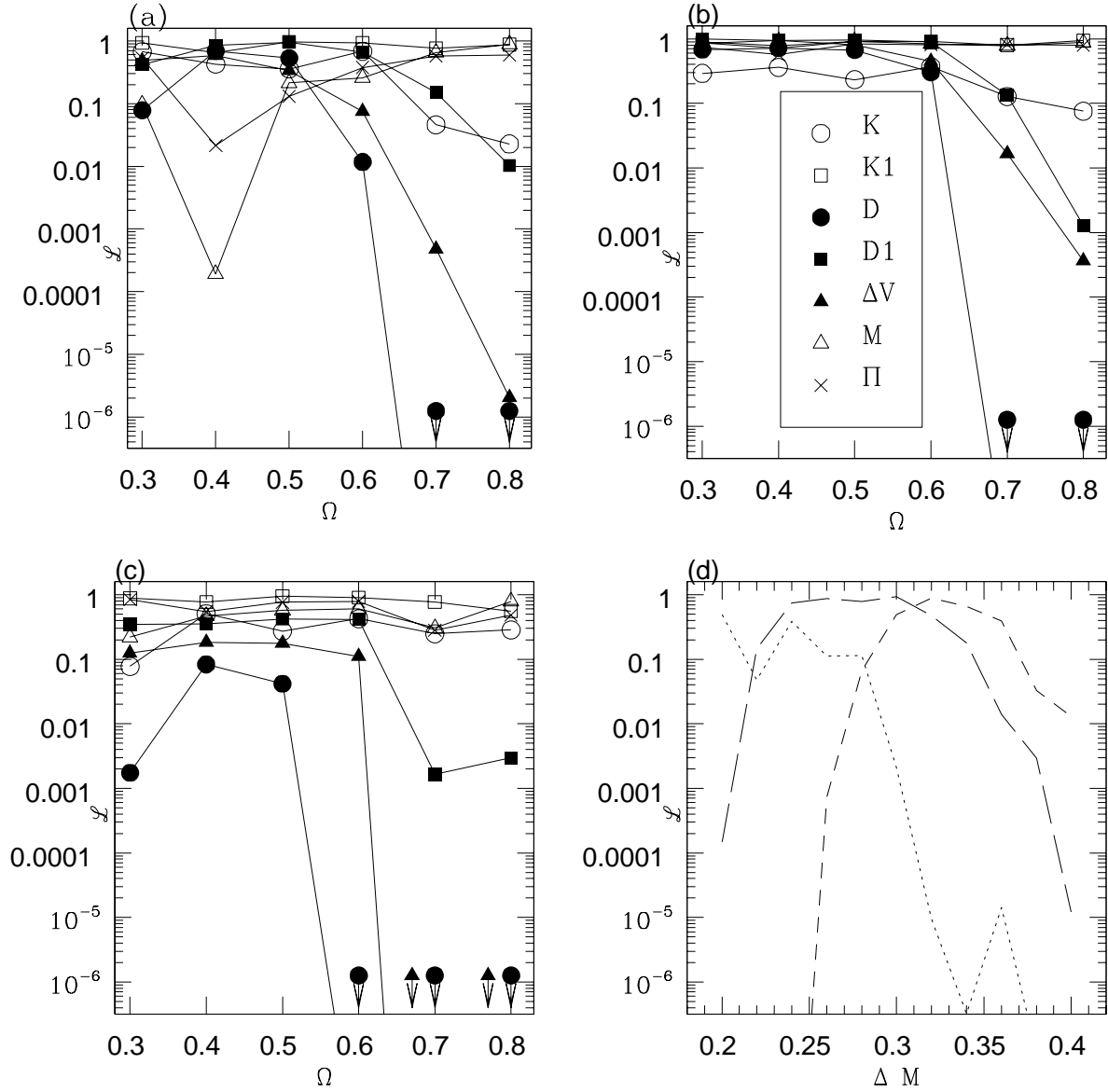


Fig. 6.— Likelihood estimates of the models for the different statistical tests (eq. 9) as a function of density parameter  $\Omega$  (figures 6a to 6c). The adopted catalog depth is  $d_{lim} = 10000$  km/s. Open circles: K, open squares: K1, filled circles: D, filled squares: D1, filled triangles:  $\Delta V$ , crosses:  $\Pi$ , and open triangles:  $M$ . Figure 6a: TF scatter  $\Delta M = 0.35$  mag considered in the mock catalogs. Figure 6b: same as figure 6a with an additional  $-0.15$  mag zero-point offset. Figure 6c: same as figure 6a with an additional  $+0.15$  mag zero-point offset. In figure 6d we show the Likelihood estimates for the open CDM models  $\Omega = 0.4$ ,  $\Omega = 0.6$  and  $\Omega = 0.8$  (dashed, long dashed and dotted lines respectively), for the  $\Delta V$  test as a function of the magnitude of the TF scatter  $\Delta M$ .